Commun. Fac. Sci. Univ. Ank. Series A2-A3
V. 46. pp. 15-22 (2001)

REAL GAMMA SCATTERING AT TESLA × N COLLIDER

M. KANTAR

Department of Physics, Faculty of Sciences and Arts, Muğla University, Muğla, TURKEY

(Received Jan. 24, 2001; Revised Feb. 02, 2001; Accepted March 28, 2001)

ABSTRACT

The proposal for measurement of polarized gluon and quark distributions in scattering of polarized real γ beam on polarized nuclear target have been considered. High energy γ beam is obtained by backscattering of laser beam off electrons from ring and linac type accelerators. Requirements for lasers and design problems are discussed.

1. INTRODUCTION

Investigations indicate that measurement of polarized gluon distribution should play a crucial role in our understanding of nucleon spin structure. To obtain a full experimental information about the spin composition of nucleon, more and better experiments are needed. We proposed an experiment ([2], [3]) to directly measure the polarized gluon distribution in the scattering of polarized real gamma beam on polarized nuclear target.

2. MAIN CONSIDERATIONS

2.1. Formation of Polarized Real Photon Beam

The polarized real photon beam is produced by scattering circularly polarized laser photons [1] off high energy electrons provided by ring (LEP, TRISTAN, HERA) or linear (SLAC, NLC) accelerators. The energy distribution of backscattered photon is [5]

$$f(\omega)=\frac{1}{E_e\sigma_c}\frac{2\pi\alpha^2}{\kappa m_e^2}\left[\frac{1}{1-y}+1-y-4r(1-r)+\lambda_e\lambda_0 r\kappa(1-2r)(2-y)\right] \quad (1)$$

where

$$y=\omega/E_e,\quad r=y/[\kappa(1-y)],\quad \kappa=4E_e\omega_0/m_e^2 \quad (2)$$

ω is the energy of the backscattered photon, λ_e and λ_0 are helicities of initial electron and laser photon and $\sigma_c=\sigma_c^0+\lambda_e\lambda_0\sigma_c^1$ is the total Compton cross section.

Fig. 1, shows the energy distribution of real photons, for $\kappa = 5$, $\lambda_0 = 1$ and different values of λ_e. Helicity of the backscattered photon is a function of its own energy

$$\lambda_\gamma(\omega) = \frac{\lambda_0(1-2r)(1-y+\frac{1}{1-y}) + \lambda_e r\kappa\left[1+(1-y)(1-2r)^2\right]}{1-y+\frac{1}{1-y}4r(1-r) - \lambda_e\lambda_0 r\kappa(2r-1)(2-y)}$$

Plotting $\lambda_\gamma(\omega)$ versus ω we see from Fig. 2 that at the highest ω value, fully polarized real photon beam is obtained in the case of opposite polarization of electron and laser photon beams.

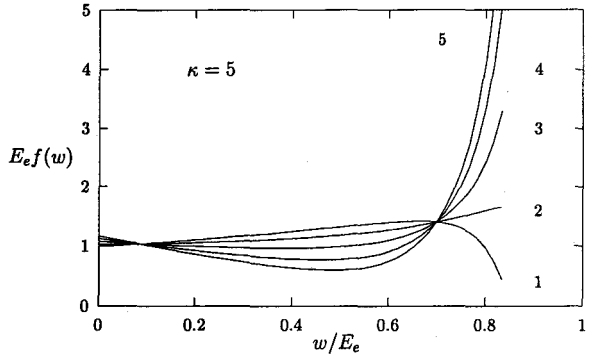

Figure 1. Energy distributions of backscattered photons. Numbers from 1 to 5 correspond to $\lambda_e\lambda_0 = 0.9, 0.5, 0.0, -0.5, -0.9$, respectively

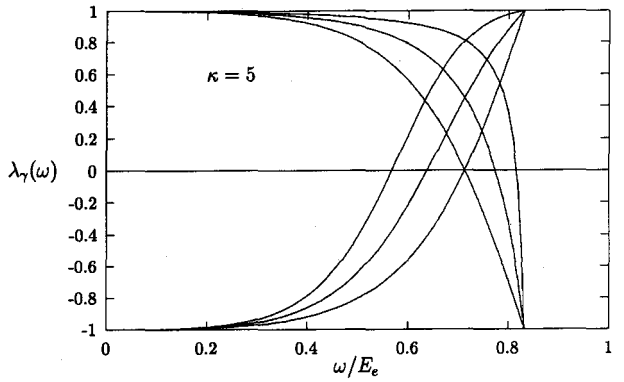

Figure 2. Helicity of backscattered photons as a function of their energy. Set of curves starting from bottom (lower set) are plotted $\lambda_0 = -1$ and those starting from the top (upper set) for $\lambda_0 = 1$. Lines from the left to right for lower set correspond to $\lambda_e = 0.9, 0.5, 0.0$ and for upper set $\lambda_e = 0.0, 0.5, 0.9$.

The maximal energy of backscattered photons $\omega_{\max} = \kappa E_e/(\kappa+1)$ will increase, in principal, up to nearly the electron beam energy. Between the IP (Interaction Point) and target a slit or collimator with a small opening is needed to select high energy photons. According to the energy dependence of photon scattering angle

$$\theta_\gamma(\omega) = \frac{m_e}{E_e}\sqrt{\frac{E_e\kappa}{\omega} - (\kappa+1)} \tag{3}$$

the highest energies have the smallest scattering angle compared to the trajectory of the incoming electron. For monochromatization i.e. $0.99\omega_{\max} \le \omega \le \omega_{\max}$, the angle $\theta_\gamma \le 1.2\mu$ rad for LEP. Taking the distance between the conversion region and the selecting slit as 100 meter, one easily obtains slit diameter $d = 360\mu m$. Compton backscattering angle θ_γ is smaller than θ_e coming from the divergence of electron beam. If a slit is used instead of collimator for monochromatization, luminosity will decrease by a factor of θ_γ/θ_e. Behind the slit an absorber and a magnet should be placed in order to sweep away any electrons, hadrons or muons produced here. After all, we have monochromatic, fully polarized γ beam coming to the target.

2.2. Number of Converted Photons

The number of converted photons n_γ is determined by the requirement of obtaining one event in each collision with the polarized target

$$\beta k n_e T_n \sigma_{\gamma p} = 1 \tag{4}$$

where β is fraction of the photons passing through the slit, T_n is density of nucleons in the target and n_e is number of electrons in a bunch. Substituting the value of total cross section of gamma-proton interaction ($\sigma_{\gamma p} \simeq 100\mu b$), n_e, thickness of our target and β in the case of 1% gamma beam monochromaticity immediately gives the number of converted photon

$$n_\gamma = kn_e$$

As long as electron bunches from the ring accelerators are used repeatedly, the smaller k the larger target thickness is preferable. In the linac case where each electron bunch is used once, keeping k larger may be more effective. So the polarized target with lower thickness can be chosen.

2.3. Luminosities

For the ring type accelerators integrated luminosity is given by

$$L^{\text{int}}_{ring} = \frac{\tau_b}{\tau_a + \tau_b + \tau_f} f_{rep}\beta\tilde{n}_e k T_n 10^7 \tag{5}$$

here, τ_a is acceleration time, τ_f is filling time, τ_b may be considered as mean lifetime of the beam, and given by

$$\tau_b = \frac{\ln(1-\delta)}{\ln(1-k)} \frac{c}{2\pi R} \tag{6}$$

where δ is maximal fraction of used electrons permitted by beam dynamics. After each collision n_e will be reduced like

$$\tilde{n}_e \approx (1 - \tfrac{l}{2} k) n_e \tag{7}$$

where l represents the number of collision. $f_{rep} = (c / 2\pi R) n_b$ is repetition rate, here c is the speed of light, $2\pi R$ is the circumference of the ring and n_b is number of bunches in the ring. Considering the above mentioned requirement, maximum integrated luminosity for ring type accelerators takes the following form

$$L_{ring}^{\max} = \frac{\tau_b}{\tau_a + \tau_b + \tau_f} f_{rep} \frac{\tilde{n}_e}{n_e} \frac{1}{\sigma_{\gamma p}}$$

For linac type accelerators, integrated luminosity is

$$L_{linac}^{\text{int}} = f_{rep} \beta k n_e T_n 10^7$$

or the maximum integrated luminosity

$$L_{linac}^{\max} = \frac{f_{rep}}{\sigma_{\gamma p}} 10^7$$

where $f_{rep} = f_{pulse} n_b$.

3. LASER PARAMETERS

Our laser has to fulfill the following requirements:

a) Repetition rate should be commensurable with frequency of electron bunches reaching the conversion region,
b) The energy of laser photons should be of the order of 1 eV,
c) Laser pulse energy would be determined by conversion coefficient.

For the linac type electron accelerators frequency of laser pulses should be commensurate with f_{rep}. In the case of multibunch accelerator mirror system should be used in order to convert all bunches accelerated in one linac pulse [4].

Let us recall the definition of the conversion factor

$$k = \frac{n_\gamma}{n_e} = \frac{A}{A_0} \tag{8}$$

where A_0 is the laser pulse energy such that each electron in a bunch is subject to collision with a laser photon and A is a pulse energy needed. The condition for each electron to be scattered once from the laser bunch is given by

$$\frac{n_0}{S_{laser}}\sigma_c = 1 \tag{9}$$

where n_0 is the number of photons in a laser pulse, S_{laser} is the transverse area of the laser bunch in the conversion region and $\sigma_c = 10^{-25} cm^2$ is the Compton cross-section of the electron. Since all electrons should pass through the laser bunch, it is clear that $S_{laser} \geq S_e = 4\pi\sigma_x\sigma_y$. Laser pulse energy A_0 is defined as $A_0 = n_0\omega_0$, here $\omega_0(1\ eV)$ is the energy of laser photon. The value of required pulse energy

$$A = kA_0$$

turns out to be in the order of μJ. In order to increase conversion efficiency, the length of laser and electron bunches must overlap in the interaction region.

4. APPLICATIONS

4.1. Processes

The proposed experiment will give opportunity to investigate wide spectrum of polarization phenomena, starting from polarized γ-nucleon total cross section to the polarized quark and gluon distributions including peripheric interactions, exclusive meson productions etc. The main subprocesses of photoproduction and corresponding final states are listed in Table 1.

Table 1. The main inclusive photoproduction processes to determine parton distributions.

Subprocesses	Final States
$\gamma q \to \gamma q$	$\gamma p \to \gamma jX$, γhX (h : light mesons)
$\gamma q \to gq$	$\gamma p \to jjX$
$\gamma g \to \bar{q}q$	$\gamma p \to jjX$, $\gamma h_1 h_2 X$
$\gamma g \to \bar{c}c$	$\gamma p \to jjX$, $\bar{D}DX$, $J/\Psi X$; $c \to s\mu^+\bar{\nu}_\mu$
$\gamma g \to \bar{b}b$	$\gamma p \to jjX$, $\bar{B}BX$, ΥX; $b \to c\mu^-\nu_\mu$, $c \to s\mu^+\bar{\nu}_\mu$

Here, we are interested in polarized parton distributions in nucleons. The information will come from heavy quark productions such as open charm, J/Ψ and Υ (at NLC) productions.

In our calculations, we used the parametrization for the helicity difference gluon distribution function [6]

$$\Delta G(x,Q_0^2) = Nx^{-0.4}(1-x)^8 \tag{10}$$

where

$$N = \Delta G(Q_0^2)/\beta(0.6,1.8) \tag{11}$$

Three sets are labeled by 1, 2 and 3 according to values of $\Delta G(Q_0^2) = 0.5$, 0.3 and 5.7 at $Q_0^2 = 4GeV^2$, respectively. The distribution can be obtained at any Q^2 by evolving it with Altarelli-Parisi equations.

The results for the asymmetry for three sets of polarized gluon distributions as a function of E_γ are ploted in Fig. 3 and Fig. 4 for J/Ψ and Υ productions respectively. Clear sensitivity to different parton parametrization can be seen.

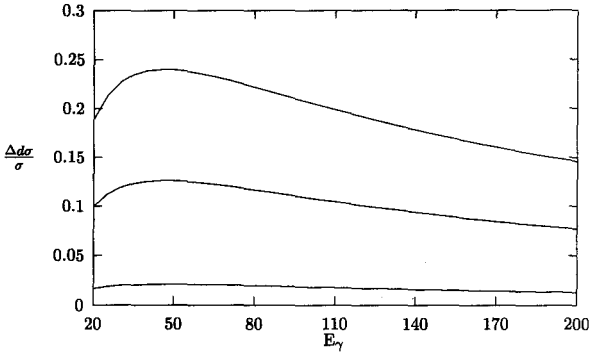

Figure 3. J/Ψ production asymmetry in polarized gamma-proton scattering for three sets of polarized gluon distributions. Curves from lowest to highest correspond to sets 1, 2 and 3, respectively.

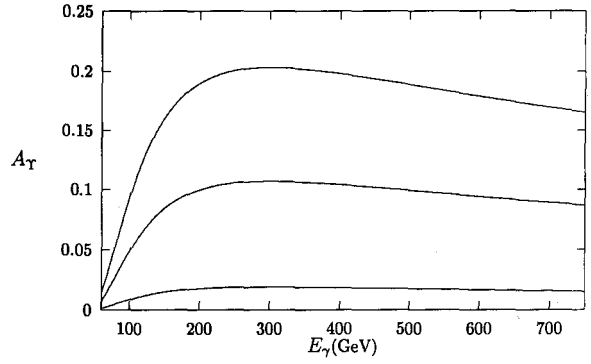

Figure 4. Υ production asymmetry in polarized gamma-proton scattering for three sets of polarized gluon distributions. Curves from lowest to highest correspond to sets 1, 2 and 3, respectively.

In the following subsection, we consider the proposed REGAS experiment for several accelerators and present the necessary parameters. Throughout the calculations we have taken $\kappa=5$ and consequently $\beta = 0.026$, $n_\gamma = 0.96\times10^4$, we used deuterated butanol target with the length about 40 cm and thickness 4×10^{25} cm^{-2}. The distance between IP and the selecting slit is taken as 100 m.

4.2. REGAS at TESLA $\times N$

The parameters of TESLA electron beam :

$E_e(TeV)$	$n_e(10^{10})$	$f_{rep}(Hz)$	n_b	$\sigma_x(nm)$	$\sigma_y(nm)$	$\sigma_z(mm)$
250	5.15	10	800	640	100	1

The parameters of the REGAS experiment :

$\omega_0(eV)$	$\theta_\gamma(\mu rad)$	$k(10^{-7})$	$A(pJ)$	L_{int}
1.3	0.51	1.86	3.1	0.8(fb^{-1})

$\sigma_{\gamma p}(\gamma p \to \Upsilon X) = 1\ nb\ at\ E_\gamma = 200\ GeV$; $N_\Upsilon = 0.8\times10^6$ 20000 $\Upsilon \to \mu^+\mu^-$.

5. CONCLUSIONS

Having almost monochoromatic and fully γ -beam, the REGAS experiment will provide advantages in investigations of polarized phenomena. When it comes to gluon polarization, at intermediate scale machines (LEP, HERA, TRISTAN, SLAC, TESLA, so on) main information will come from J/Ψ and open charm bottom productions will be more advantageous.

ACKNOWLEDGEMENTS

I would like to thank TUBITAK for giving financial support to visit Fermilab in U.S. and also thank High Energy Physics Group at Ankara University for useful discussions.

REFERENCES

[1] Anderson, S.G., Laser Parameters Handbook, Laser Focus World (1996).
[2] Alekhin, S.I., Borodulin, V.I. and Sultansoy, S., Inter. J. of Modern Phys. A 8 (1993) 1603.
[3] Atağ, S. et al., Europhysics Lett 29 (1995) 273; Turkish J. of Physics 19 (1995) 815; Nucl. Instr. and Meth. A 381 (1996) 23.
[4] Çiftçi, A.K. et al., Nucl. Instr. and Meth. A 365 (1995) 317.
[5] Ginzburg, I.F. et al., Nucl. Instr. and Meth. 205 (1983) 47; ibid. 219 (1984) 5; Telnov, V.I., Nucl. Instr. and Meth. A 294 (1990) 72; Borden, D.I., Bauer, D.A. and Caldwell, D.O., SLAC Preprint SLAC-PUB-5715, Stanford (1992).
[6] Keller, S. and Owens, J.F., Phys. Rev. D 49 (1994) 1199.